Electron Transport Behavior of Multiferroic Perovskite $BiMnO_3$ Prepared by Co-Precipitation Method *

Hong-Jun Wang(王红军), Yuan-Yuan Zhu(朱媛媛)**, Jing Zhou(周静)

Department of Physics, Shaanxi University of Science and Technology, Xi'an 710021

(Received 10 October 2017)

Perovskite $BiMnO_3$ samples are successfully synthesized by the co-precipitation method at relatively low pressure and moderate temperature. The temperature dependences of resistivity are measured and systematically investigated. It is shown that the electrical resistivity increases sharply with the decrease of temperature above 210 K and the fitted results demonstrate that the thermally activated conduction model is the dominant conduction mechanism for the electron transport behaviors in this temperature region. A dual conducting mechanism, i.e., the variable range hopping and thermal activated conduction, is suggested to be responsible for the transport behaviors of $BiMnO_3$ in the region of 180–200 K. Moreover, the resistivity increases slightly with the decrease of temperature below 180 K and the transport is governed by the variable range hopping mechanism.

PACS: 72.80.Ga, 72.15.Eb, 66.70.Df DOI: 10.1088/0256-307X/35/2/027201

Multiferroic $BiMnO_3$ has been widely studied because it possesses ferromagnetic and ferroelectric properties simultaneously.[1,2] As a result, it is highly important in applications in multifunctional devices.[3–5] $BiMnO_3$ shows three different crystalline structures depending on the ambient temperature. It reveals a high distorted perovskite-type monoclinic phase I (space group: $C2/c$) at temperature below 474 K, a monoclinic phase II (space group: $C2$) in the region of 474–768 K and an orthorhombic phase (space group: $Pnma$) above 768 K up to the decomposition temperature, respectively.[6,7]

$BiMnO_3$ has been synthesized by various methods.[8] Bulk $BiMnO_3$ samples can be synthesized only at high pressure ($P > 3$ GPa) and high temperature ($T \sim$ 500℃–700℃). $BiMnO_3$ has metastable characteristics at low pressure or under ambient conditions.[9–11] This situation makes it a hard material for fundamental research. In the present work, systematic efforts are made to synthesize $BiMnO_3$ compounds by the co-precipitation method with a high purity at low pressure and moderate temperature.

$BiMnO_3$ exhibits the semiconductor behavior in a wide temperature region. However, the mechanisms for the electron transport behaviors of $BiMnO_3$ are still in debate. For example, some researchers suggested that the thermally activated conduction mechanism is responsible for the transport behavior.[12] As a contrast, others believed that it is the variable range hopping (VRH) mechanism which governs the electron transport behavior.[13]

To understand the underlying physical mechanisms for the electron transport behavior of $BiMnO_3$ more clearly, further systematical works are very important and necessary. In this work, temperature dependences of resistivity in perovskite $BiMnO_3$ are systematically investigated. To our interest, in the temperature region above 210 K, the thermally activated conduction mechanism is responsible for the transport behavior of $BiMnO_3$. The transport behavior in the region of 180–200 K can be well explained with a dual mechanism: the thermally activated conduction and the VRH conduction. It is found that the electron transport behavior below 180 K is governed by the VRH mechanism. Our results indicate that the electron transport behavior of $BiMnO_3$ may result from the combined effects of different conduction mechanisms.

The $BiMnO_3$ samples were synthesized by the co-precipitation method with bismuth oxide (Bi_2O_3), manganese chloride ($MnCl_24H_2O$), sodium hydroxide (NaOH), concentrated nitric acid (HNO_3) and polyglycol as reactants. All the chemicals used in this work were analytical grade and the distilled water was used as the solvent throughout the experiment.

First, the distilled water and concentrated HNO_3 with the volume ratio of 1:2 were used for the preparation of dilute HNO_3. Bi_2O_3 and $MnCl_24H_2O$ in stoichiometric proportion (1:2 mole ratio) were dissolved in the sequence of dilute HNO_3 and polyglycol (5% mass fraction), respectively. An excess aqueous NaOH was drop-wise added into the mixed solution to precipitate the hydroxides of manganese and bismuth. To ensure the complete precipitation process, the PH value of the mixed solution should reach twelve. Furthermore, the color of the precipitate changed from white to brown gradually during the precipitation process. Finally, the mixture was transferred to a distillation flask and then sealed with a magnetic stirrer at 100℃ under constant stirring for 6 h. Eventually, the mixture was filtered until the solution was neutral.

*Supported by the Key Research Project of Shaanxi University of Science and Technology under Grant Nos 2016GBJ-12 and 2016BJ-59.

**Corresponding author. Email: zhuyuanyuan@sust.edu.cn

The precipitate was dried in the oven all day. The powders were then pressed into pellets, and heated in 300℃ for 3 h.

X-ray diffraction (XRD) measurement with Cu radiation at a scanning rate of $0.02\,s^{-1}$ was employed to characterize the crystalline structure of $BiMnO_3$ samples at room temperature. The chemical bonding states were revealed by the x-ray photo electron spectroscopy (XPS) with Mg excitation. Scanning electron microscope (SEM) was employed to investigate the morphology of the $BiMnO_3$ samples. Resistivity measurements were carried out by the physical property measurement system (PPMS 6000, Quantum Design, USA) with the common four-probe method.

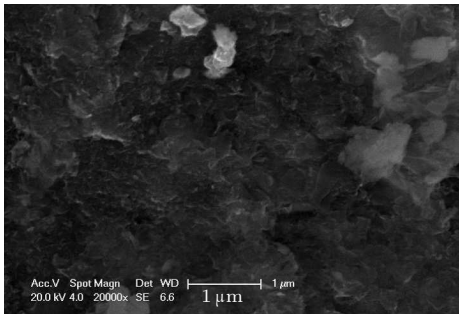

Fig. 1. SEM image of $BiMnO_3$ samples.

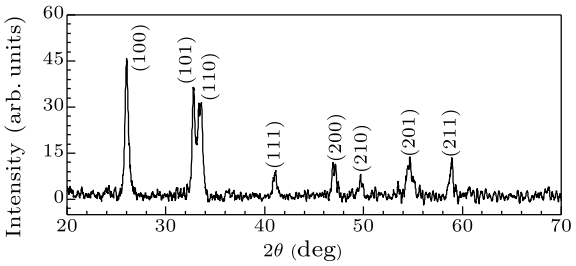

Fig. 2. The XRD patterns of $BiMnO_3$ samples carried out at room temperature.

Figure 1 shows the SEM image of the $BiMnO_3$ samples. It is noted that the dense $BiMnO_3$ samples comprising nanoparticles are observed. To investigate the crystalline structure of the $BiMnO_3$ samples, the XRD measurements were carried out at room temperature. Figure 2 displays the typical XRD patterns of the polycrystalline $BiMnO_3$ sample. The prominent peaks presented in Fig. 2 show relatively small width at half maximum (FWHM), indicating the formation of the crystalline phase. Furthermore, the low background and sharp peaks results also suggest the high crystallinity of the $BiMnO_3$ sample.

The patterns include eight obvious diffraction peaks and all those observed reflection peaks can be readily indexed to the pure monoclinic (Space group: $C2/c$) structure with lattice parameters of $a = c = 3.935$ Å, $b = 3.989$ Å and $\beta = 91.0°$.[14] It is noted that this XRD profile is in good agreement with that in the reported work.[15] The results indicate that this co-precipitation method can facilitate the formation of pure $BiMnO_3$ sample with relatively homogeneous morphology.

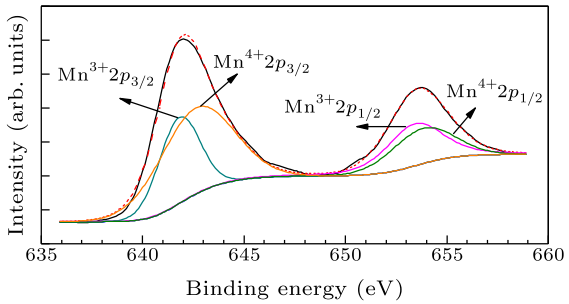

Fig. 3. Typical XPS spectrum of Mn $2p$ region for the $BiMnO_3$ sample.

XPS was used to characterize and analyze the chemical state of manganese element in the $BiMnO_3$ sample. The experimental spectrum is reported (black solid) together with result of total curve fitting (red dash-dotted). Moreover, the dark cyan, magenta, olive and orange lines are referred to the fitted results of Mn^{3+} $2p_{3/2}$, Mn^{3+} $2p_{1/2}$, Mn^{4+} $2p_{1/2}$ and Mn^{4+} $2p_{3/2}$, respectively (Fig. 3). It is noted that the Mn $2p$ doublet is composed of two fitted doublet lines. It is assigned to Mn^{3+} and Mn^{4+}, respectively. The fitting results show that the atom ratio Bi:Mn:O=1:1:3.29, indicating the existence of interstitial oxygen ions in $BiMnO_3$.

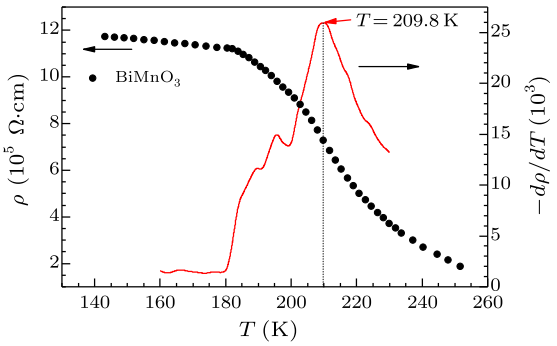

Fig. 4. Temperature dependence of electrical resistivity (black points) and $d\rho/dT$ (Ω·cm/K) curves (red line) for the $BiMnO_3$ sample.

Figure 4 shows the temperature dependences of electrical resistivity (ρ) of the $BiMnO_3$ sample in the temperature range of 140–260 K. It is noted that the electrical resistivity decreases with increasing temperature in the whole measured temperature range. A clear upward inflection near 210 K can be observed in the resistivity versus temperature curve (the conversion temperature is defined as the temperature at which the $d\rho/dT$ curve has the maximum slope). The resistivity is in an order of $\sim 10^5\,\Omega$·cm at 26 K, which is much lower than the previously reported value.[16] This low resistivity indicates the presence of a significant amount of Mn^{4+} cations,[13] which is affirmed by the results of XRS spectrum (Fig. 3). In the temperature region above 210 K, the electrical resistivity

increases sharply with the decrease of temperature. As the temperature goes below 210 K, the resistivity increases slightly with decreasing temperature and it eventually reaches a magnitude order of $\sim 10^6\,\Omega\cdot$cm.

The electrical resistivity upward inflection near 210 K means that the conversion of electron transport behavior for perovskite $BiMnO_3$ occurs at ~210 K. For a more intuitive observation of the resistivity change trend, the $d\rho/dT$ ($\Omega\cdot$cm/K) versus T curve of the $BiMnO_3$ sample is re-plotted in Fig. 4 (red line). It is found that the curve shows an obvious peak at ~210 K. It is noted that this peak is sharp and steep. The curve becomes flatter as the temperature goes below 180 K.

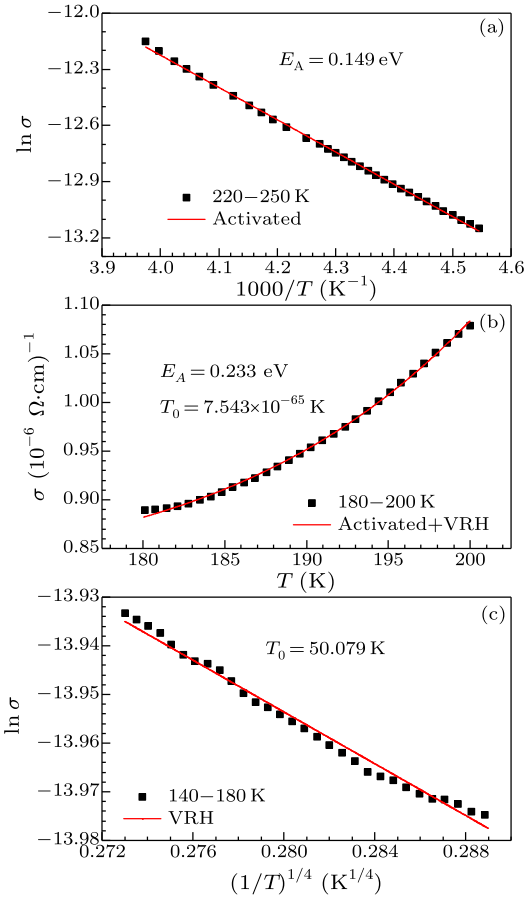

Fig. 5. Fitted results of the conductivity versus temperature of $BiMnO_3$, (a) above conversion temperature by the activated model, (b) in the temperature region 180–200 K by the two-mechanism model, (c) below 180 K by the three-dimensional VRH model.

The underlying mechanism for the electron transport behavior of perovskite $BiMnO_3$ is an interesting issue. Firstly, the electron transport behavior above the conversion temperature of 210 K is investigated. The results show that the electrical resistivity of $BiMnO_3$ exhibits a rapid increase trend with decreasing temperature, indicating the semiconductor behavior of $BiMnO_3$ without controversy. We try to fit the result using the thermally activated conduction model in the temperature region above the conversion temperature of 210 K. For the thermally activated conduction, the conductivity (σ) can be expressed as $\sigma_{\rm activated} = A\exp(-E_{\rm A}/kT)$, where $E_{\rm A}$ is the activation energy, and k is the Boltzmann constant.[17] The activation energy $E_{\rm A}$ with a value of 0.149 eV is calculated from the Arrhenius plot of $\ln\sigma$ versus $1000/T$ (Fig. 5(a)). However, $E_{\rm A}$ for the stoichiometric $BiMnO_3$ is estimated at 0.26 eV,[18] which is higher than our results. It is well known that the electronic structure and electrical properties of $BiMnO_3$ are related to its oxygen defects.[19] The DOS calculations indicate that the interstitial oxygen ions in $BiMnO_3$ decrease the activation energy.[20,21] Therefore, we can expect that the existence of the interstitial oxygen ions in our $BiMnO_3$ sample results in the lower activation energy, as indicated by the XPS results in Fig. 3.

Secondly, the electron transport behavior of $BiMnO_3$ in the temperature range of 180–200 K is discussed. Our attempts to fit the transport behavior using the simple activated or VRH model have failed. It seems that no single conduction model could accurately describe the electron transport behavior of $BiMnO_3$ samples in this discussed temperature range. To explain the electron transport behaviors of $NdNiO_3$, Catalan *et al.*[22] have proposed a model by assuming that more than one mechanism plays a role simultaneously for the electron transport behavior. Moreover, $MgTi_2O_4$ and its La-doped counterparts have also been successfully interpreted for their electrical behavior by the dual conduction mechanism model.[23] We try to fit the temperature dependences of conductivity in this temperature region by considering two different contributions: one is from the contribution of thermal activated behavior; and the other is from the contribution of VRH behavior. In the fitting, the thermal activated conductivity takes the form of $\sigma_{\rm activated} = A\exp(-E_{\rm A}/kT)$ and the VRH conductivity takes the form of $\sigma_{\rm VRH} = B\exp[-(T_0/T)^{1/4}]$, where $T_0 = (2.587)^4/N(E_{\rm F})R^3k$ with $N(E_{\rm F})$ being the density of the states around the Fermi level, $\sigma_{\rm VRH}$ is the VRH distance, $E_{\rm A}$ is the thermal activation energy, and k is the Boltzmann constant.[17,24,25] It can be seen from Fig. 5(b) that the relationship between conductivity and temperature in the temperature range of 180–200 K meets the formula of $\sigma(T) = \sigma_{\rm activated} + \sigma_{\rm VRH} = A\exp(-E_{\rm A}/kT) + B\exp[-(T_0/T)^{1/4}]$ very well. The fitting parameters are $E_{\rm A} = 0.233$ eV and $T_0 = 7.543\times10^{-65}$ K. It is noted that the thermal activation energy in this temperature region is higher than that above the conversion temperature of 210 K. This is due to the reason that the higher energy is needed for the electron transport behavior in this low temperature region.

Eventually, the slightly increasing resistivity with decreasing temperature also demonstrates the semiconductor state of the $BiMnO_3$ sample below 180 K. We try to fit it with the VRH law $\sigma = B\exp[-(T_0/T)^{1/4}]$.[23–26] It is found that the VRH model can fit the experimental data well at tempera-

tures below 180 K, as shown in Fig. 5(c), with a fitting parameter of $T_0 = 50.079$ K. As a result, the resistivity behavior versus temperature for $BiMnO_3$ below 180 K can be explained by the VRH electron transport mechanism. According to this behavior, the $Mn^{3+}OMn^{4+}$ complex allows electron-hopping conduction by the double exchange mechanism.[13]

In summary, perovskite $BiMnO_3$ samples have been synthesized by the co-precipitation method and the corresponding electron transport behavior is systematically discussed. To give a more general insight into the transport behavior, the temperature dependences of conductivity are fitted using different conducting mechanisms. The electron transport behavior above 210 K is governed by the thermally activated conduction mechanism, and the VRH conduction mechanism is responsible for the behavior below 180 K. Moreover, the transport behavior of the $BiMnO_3$ system in the temperature range of 180–200 K results from the combined effects of the VRH and thermally activated conduction.

References

[1] Son J Y, Park C S and Kim H 2010 *Met. Mater. Int.* **16** 289
[2] Yao C D, Gong J F, Geng F F, Gao H, Xu Y L, Zhang A M, Tang C M and Zhu W H 2010 *Acta Phys. Sin.* **59** 5332 (in Chinese)
[3] Li S, Zhang J M, Kibria M G et al 2013 *Chem. Commun.* **49** 5856
[4] Shirolkar M M, Hao C, Dong X et al 2014 *Nanoscale* **6** 4735
[5] Mukherjee A, Basu S, Manna P K et al 2014 *J. Mater. Chem. C* **2** 5885
[6] Brankovi Z, Stanojevi Z, Mancic L et al 2010 *J. Eur. Ceram. Soc.* **30** 277
[7] Yokosawa T, Belik A A, Asaka T et al 2008 *Phys. Rev.* B **77** 024111
[8] Lee B W, Yoo P S, Nam V B et al 2015 *Nanoscale Res. Lett.* **10** 47
[9] Guennou M, Bouvier P, Toulemonde P et al 2014 *Phys. Rev. Lett.* **112** 075501
[10] Sugawara F and Iiida S 1968 *J. Phys. Soc. Jpn.* **25** 1553
[11] Belik A A, Matsushita Y, Tanaka M et al 2011 *Inorg. Mater.* **50** 7685
[12] Eerenstein W, Morrison F D, Scott F et al 2005 *Appl. Phys. Lett.* **87** 101906
[13] Dar M S and Akram K B 2014 *J. Supercond. Novel Magn.* **27** 613
[14] Mazumder N, Uddin I, Khan S et al 2007 *J. Mater. Chem.* **17** 3910
[15] Sun B and Li C M 2015 *Phys. Chem. Chem. Phys.* **17** 6718
[16] Grizalez M, Delgado E, Gómezand M E and Prieto P 2007 *Phys. Stat. Sol.* **4** 4203
[17] Majumdar S and Banerji P 2010 *J. Appl. Phys.* **107** 063702
[18] Chiba H, Atou T and Syono Y 1997 *J. Solid St. Chem.* **132** 139
[19] Woo H, Tyson T A and Croft M et al 2001 *Phys. Rev.* B **63** 134412
[20] Seshadri R and Hill N A 2001 *Chem. Mater.* **13** 2892
[21] Koronska R B and Nalecz D M 2013 *Phase Trans.* **86** 167
[22] Catalan G, Bowman R M and Gregg J M 2000 *Phys. Rev.* B **62** 7892
[23] Zhu Y Y, Wang H J, Wang L, Liu Y, Xiong R and Shi J 2016 *J. Alloy Compd.* **666** 248
[24] Zhu Y Y, Wang R J, Wang L, Liu Y, Xiong R, Shi J, An L H and Sun D H 2014 *Chin. Phys. Lett.* **31** 097201
[25] AnisurRahman K M, Schneider S C and Seitz M A 2005 *J. Am. Ceram. Soc.* **80** 1198
[26] Belik A A 2017 *J. Solid State Chem.* **246** 8